

DEVELOPING NANOCELLULOSE-BASED BIOFILMS FROM KRAFT AND NaBH_4 -MODIFIED KRAFT PULP

AYHAN TOZLUOGLU,* BAYRAM POYRAZ,**
ARMANDO G. MCDONALD*** and ZEKI CANDAN****

**Department of Forest Products Engineering, Faculty of Forestry, Duzce University,
81620 Duzce, Turkey*

***Department of Polymer Engineering, Faculty of Technology, Duzce University
81620 Duzce, Turkey*

****Renewable Materials Program, Department of Forest, Rangeland and Fire Sciences,
University of Idaho, Moscow, Idaho 83844-1132, USA*

*****Department of Forest Products Engineering, Faculty of Forestry, Istanbul University, 34473
Istanbul, Turkey*

✉ *Corresponding author: Zeki Candan, zekic@istanbul.edu.tr*

Received May 23, 2017

In this study, both kraft pulp and NaBH_4 -modified kraft pulp produced from the red gum tree (*Eucalyptus camaldulensis*) were used to generate nanofibrillated cellulose (CNF) and microfibrillated cellulose (CMF). These were then characterized by HPLC, FTIR, DSC and ^{13}C -NMR. Morphological and viscoelastic properties were investigated *via* SEM and rheometry, respectively. The storage moduli of the biofilms produced from the CNFs were investigated by dynamic mechanical thermal analysis (DMTA). Some minor shifts were observed in the ^{13}C -NMR for the CMF and CNF obtained from NaBH_4 -modified kraft pulp. The CMF and CNF obtained from kraft pulp revealed higher thermal stability due to higher crystallinity. Higher dynamic mechanical properties were seen in the CNF film obtained from kraft pulp and the results were useful in ascertaining its potential application value.

Keywords: biofilm, enzyme, CMF, CNF, NaBH_4

INTRODUCTION

The growing interest in environmentally friendly materials has extended to industrial research. Cellulose is one of the lignocellulosic materials and consists of a hierarchical fibrillar structure that forms elemental molecular chains, which are further organized into the larger constituents of microfibrils and macrofibrils. As for the molecular structure, it is composed of anhydroglucose units linked at the first and fourth carbon atoms by β -glycosidic bonds. Cellulose has been promoted as a natural polymer owing to its renewable and biodegradable properties and its mechanical robustness.¹ Microfibrillated cellulose (CMF), nanofibrillated cellulose (CNF), nanocrystalline cellulose (CNC) and bacterial cellulose (BC) are outstanding regenerated cellulose materials.

Microfibrillated cellulose, with fibrils of 1-50 nm in diameter and several μm long, pioneered by Sandberg *et al.*² in the late 1970s and early 1980s, was produced through the wood pulp fiber homogenization process of Turbak *et al.*³ Although this type of cellulose was regarded as CNF by Garrasco⁴ due to the composition of the nanofibrils, fibrillar fines, fiber fragments and fibers, it was not considered as CNF by Kumar *et al.*⁵ Therefore, the terms CMF and CNF have been used differently in the literature in reference to these materials.

Nanocrystalline cellulose (width of 5-70 nm, length of 100 nm-several μm) is generated by using a treatment with strong acids to remove amorphous sections.⁶ However, cellulose nanofibers are more effective than cellulose nanocrystals in increasing the viscoelasticity of hydrogels due to the entanglement provided by the nanofibers.⁷ The aforementioned properties of CMF have led to a wide range of applications, including as a low-calorie thickener and suspension stabilizer in food products⁸ and in cosmetics and pharmaceuticals.⁹ Due to the absorptive and strength properties of the finely divided cellulose, it is also used in sanitary products,¹⁰ wound dressings¹¹ and coating agents.¹² It is also employed as a component in medicinal tablets,¹³ regenerated-cellulose products¹⁴ and in battery separators.¹⁵

Furthermore, new composites with improved mechanical and optical properties have been produced by reinforcing neat polymers with CMF, CNF and CNC.¹⁶⁻¹⁸ CMF exhibits excellent mechanical properties, besides being translucent and reactive due to the larger fiber surface. Azizi Samir *et al.*¹⁹ compared the mechanical properties of CMF and CNC on polybutylacrylate (PBA) latex and polycaprolactone (PCL) and concluded that CMF, on both PBA latex and PCL, displayed superior properties as reinforcement material. In another study, CMF films impregnated with epoxy resulted in transparent composites with excellent thermal conductivity.²⁰ On the other hand, Grüneberg *et al.*²¹ revealed that the modulus of elasticity and tensile strength of neat polymers increased after the addition of CNC, whereas the extensibility of the composites was generally reduced.

The production of CMF is carried out by mechanical techniques, such as microfluidizer and super-grinding/refiner-type treatments, combinations of beating, rubbing and homogenization, high-shear refining and cryogenic crushing, ultrasonication and high-pressure homogenization.²²⁻²⁶ However, although the high-pressure homogenization process has become prominent, it is not possible to make exact comparisons to determine which types of mechanical treatment are better. Clogging and excessive energy consumption during mechanical treatment are major problems. To breach this gap, new approaches and different kinds of pretreatment are of vital importance. Therefore, several procedures have been proposed, such as a combination of enzymatic or chemical pretreatments in advance of mechanical disintegration.²²

The aim of this study was to produce CMF and CNF from kraft and NaBH₄-modified kraft pulp, which were then treated with an enzyme (Celluclast 1.5 L). There is very limited information in the literature on the effect of this enzyme. Chemical, rheological, morphological and thermal properties of CMF and CNF were examined in this study. In addition, CNF films were produced and subjected to dynamic mechanical thermal analysis (DMTA) and morphological property assessments.

EXPERIMENTAL

Materials

For this study, freshly cut logs of a 16-year-old river red gum tree (*Eucalyptus camaldulensis*) brought from Tarsus, Turkey, were used as raw material. After the bark and cambium had been carefully stripped off, the logs were reduced to 3-8 mm × 2-3 cm chips, suitable for the kraft and kraft-NaBH₄ pulping procedures. In order to assure a uniform size throughout pulping, the chips were passed through a screen after air drying.

The enzyme employed to break down the cellulose and hemicellulose structures was Celluclast 1.5 L, a cellulase in which 1,4-beta-D-glucosidic linkages are hydrolyzed in cellulose and other beta-D-glucans (Novozymes, Bagsvaerd, Denmark).²⁷ In addition, cellulase hydrolyses the cellulose chain internally and liberates glucose units.

Methods

Pulping and bleaching

In this study, kraft and kraft-NaBH₄ pulps were utilized as cellulose sources to produce CMF and CNF (Fig. 1). The calculated H-factors were 410 and 408 for kraft and kraft-NaBH₄ pulps, respectively. The resulting pulps were broken up and washed with hot tap water, and then screened by employing a flat laboratory screen (Somerville Flat Screen, Techlab Systems) with a slot width of 0.15 mm (Tappi T275). As found in an earlier study by the authors, the kraft-NaBH₄ pulp had a lower pulp yield, kappa number and viscosity. The yields of the kraft and kraft-NaBH₄ pulps were 45.7% and 45.3% (o.d. chip), respectively. The kappa numbers of the kraft and kraft-NaBH₄ pulps were 18.4 and 14.5, respectively. In addition, the viscosities of the kraft and kraft-NaBH₄ pulps were 10.2 and 9.85 cP, respectively.²⁸

The pulps were bleached using elemental chlorine-free (ECF) processes (ODEP: oxygen-chlorine dioxide-alkaline-peroxide) (Fig. 1). After each bleaching operation, the pulps were washed with water, squeezed and crumbled. The chemical compositions of bleached kraft and kraft-NaBH₄ pulps were examined in a previous study,²⁸ where the glucan contents were found to be 66.3% and 66.2% and the xylan contents – 14.3% and 15.8% (w/w), respectively. Mannan, arabinan and galactan accounted for only 0.67% and 0.56% (w/w) of the bleached kraft and kraft-NaBH₄ pulps, respectively (Table 1).

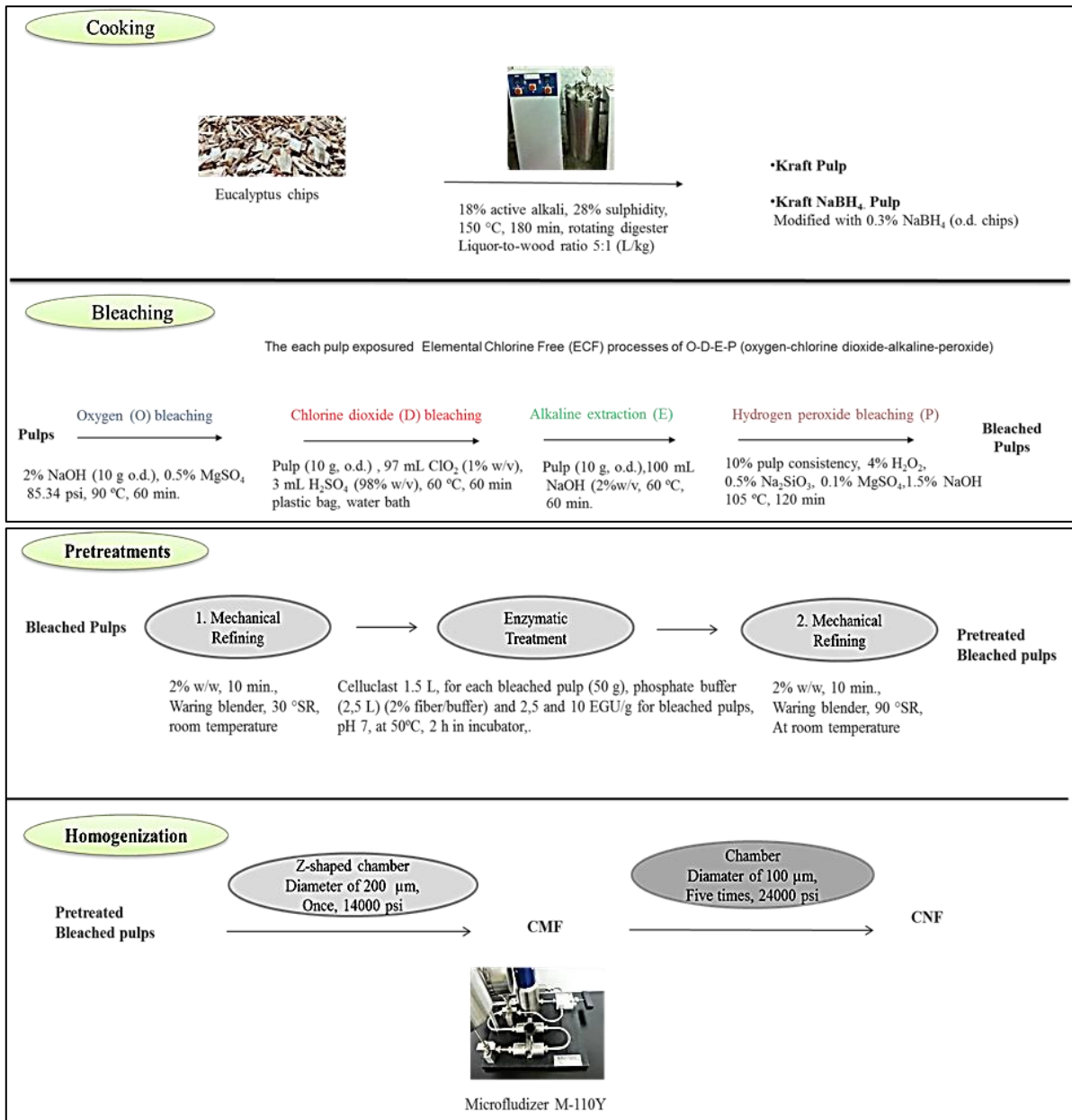


Figure 1: Experimental design for CMF and CNF production

Table 1
Chemical composition of kraft and kraft-NaBH₄ pulps after pulping and bleaching²⁸

Chemical components (%)	Chip	Kraft	Kraft-NaBH ₄	Kraft (ODEP)	Kraft-NaBH ₄ (ODEP)
Glucan	40.0 ± 1.53	61.8 ± 2.04	62.6 ± 2.04	66.3 ± 0.90	66.2 ± 0.81
Xylan	8.67 ± 0.19	15.3 ± 0.65	15.8 ± 0.65	14.3 ± 0.85	15.8 ± 0.85
Galactan	0.18 ± 0.14	-	0.10 ± 0.03	-	-
Mannan+arabinan	0.44 ± 0.20	0.33 ± 0.00	0.33 ± 0.00	0.67 ± 0.00	0.56 ± 0.20
Acid insoluble lignin (AIL)	27.6 ± 0.99	1.98 ± 0.54	1.65 ± 0.69	0.40 ± 0.09	1.28 ± 0.05
Acid soluble lignin (ASL)	0.74 ± 0.01	1.05 ± 0.02	1.07 ± 0.03	1.16 ± 0.41	1.08 ± 0.01
% Removed material (o.d. chip)					
Total material	-	54.4	54.7	58.5	60.5
Glucan	-	29.5	29.1	31.2	34.6
Xylan	-	19.5	17.4	31.6	28.0
Total lignin	-	95.1	95.7	97.7	96.7

Pretreatments and homogenization

In this stage, pretreatments and homogenization procedures were applied (Fig. 1) to produce CMF and CNF. Both bleached kraft and kraft-NaBH₄ pulps were first mechanically refined and then enzymatically (Celluclast 1.5 L) pretreated. In the enzymatic pretreatment stage, the optimum enzyme concentration was determined according to the ratio of removed glucan to xylan. The sample with the highest amount of xylan was selected for further analysis. The samples showing optimum parameters were then exposed to the second mechanical refining. After the pretreatments, the homogenization process was carried out to obtain CMF and CNF samples.

In the homogenization stage, all the pretreated bleached kraft and kraft-NaBH₄ pulps were passed through a high-pressure fluidizer (2% w/w) (Microfluidizer M-110Y, Microfluidics Corp.). For the CMF production, samples were passed once through a Z-shaped chamber with a diameter of 200 μm (14000 psi). For the CNF production, samples were passed once through a Z-shaped chamber having a diameter of 200 μm (14000 psi) and then passed five times through a chamber with a diameter of 100 μm (24000 psi).

Film manufacturing procedure

For manufacturing CMF or CNF films, the CMF or CNF was stirred for 1 h at room temperature to ensure homogeneous consistency. The CMF or CNF suspension was poured onto a glass plate. The materials were placed in a dryer to allow water evaporation at 60 °C overnight. The CNF or CMF films were peeled off the plate and kept at room temperature for 24 hours before the dynamic mechanical thermal analysis (DMTA).

Analytical methods

HPLC (high-performance liquid chromatography) analysis

The sugar contents of the suspensions were determined by Laboratory Analytical Procedures (LAP) from the National Renewable Energy Laboratory (NREL).²⁹ The sugar contents were analyzed using an HPLC system (Agilent 1200 System, Agilent Tech.) equipped with a Shodex SP0810 column (mobile phase: HPLC grade water, filtered (0.2 μm) and degassed; injection volume: 20 μL; flow rate: 0.6 ml/min; column temperature: 80 °C) and a refractive index detector.

The reduction in glucan was calculated based on the initial dry weight of the glucan in the chip/bleached kraft or kraft-NaBH₄ pulp (GU) and the dry weight of the glucan in the remaining solids after the pulping, bleaching, refining, enzymatic hydrolysis and homogenizing treatments (GP). The percentage of glucan reduction was calculated with the following equation:

$$\text{The percentage of glucan reduction} = \frac{GU - GP}{GU} \times 100 \quad (1)$$

The solubilization of xylan during the treatments was also calculated in the same manner. Furthermore, the percentage of the solids recovered was calculated on an oven-dry basis as follows:

$$\text{The percentage of solids recovered} = \frac{W2}{W1} \times 100 \quad (2)$$

where W1 is the dry weight of the whole biomass before treatment (g), and W2 is the dry weight of the treated material (g).

FTIR (Fourier transform infrared) spectroscopy

The IR spectra were taken *via* an attenuated total reflectance (ATR)-FTIR device (Shimadzu IR Prestige-21, Shimadzu Corp.). Suspensions of 0.5 ml were prepared in a concentration of 2% (w/w). The suspensions were gently dropped in a diamond attachment using an automatic pipette (0.1-1 ml). In order to elucidate molecular vibration signals in the range of 4000-600 cm⁻¹, 20 scans with a resolution of 4 cm⁻¹ were taken.

¹³C CP/MAS NMR (cross polarization magic angle spinning nuclear magnetic resonance) spectroscopy

The solid state ¹³C CP/MAS NMR spectra of the suspensions were recorded using an Advance III 300-MHz NMR instrument (Bruker Corp.). The operating frequency was fixed at 75.385 MHz. A double air-bearing probe and a zirconium oxide rotor (4 mm) were used in the analysis. The MAS rate was 8500 Hz. A CP pulse was ramped at a contact pulse of 100 μs with the rotation of 4 μs proton at 90° pulse (294.8 °K). The delay between repetitions was 2.5 s. ¹³C data were processed offline using mestReNova processing software with a line broadening of 10 Hz. Cellulose crystallinity index (CrI) was calculated from the areas of the crystalline and amorphous C4 signals using the following formula:³⁰

$$\text{CrI} = \frac{A_{86-92 \text{ ppm}}}{A_{79-86 \text{ ppm}} + A_{86-92 \text{ ppm}}} \quad (3)$$

Rheological measurements

In order to determine the rheological properties of the suspensions, an RST-CPS Rheometer (Brookfield Corp.) was used. The measurements were made at the 37.5 mm diameter cone-plate and the 25 mm diameter parallel plate. The gap was fixed at 1 mm. Before the measurements, shearing was applied to the materials at 20,000 rpm for 2 min (IKA T18 homogenizer, IKA Lab.) to disrupt any flocculated aggregates and the samples were then allowed to rest for 3 min.

SEM (scanning electron microscopy)

The morphological properties of the suspensions and films were analyzed by taking SEM (FEI Quanta FEG 250, FEI Corp.) images. The samples were first dried at 105 °C overnight, and then coated up to 5 nm with a gold-palladium composite. Pictures were taken for all the samples at 1-15 kV using a field emission gun equipped with a compacted secondary electron detector. Scales were selected as 100 μm for fiber materials and 1 and 100 μm for CMF and CNF. In addition, SEM analyses were carried out for CMF or CNF films.

Thermal analysis

The thermal properties of the suspensions were examined using differential scanning calorimetry (DSC). For the DSC, samples of approximately 3-5 mg of material were first squeezed, and then placed in an aluminum pan. In the device chamber, the sample was heated from room temperature to 500 °C at a rate of 10 °C min⁻¹. All the measurements were carried out under nitrogen flow (75 mL min⁻¹) using a Shimadzu DSC-60 Plus (Shimadzu Corp.) equipped with a thermal analysis data station. The heat flow was recorded as a function of the temperature.

Dynamic mechanical thermal analysis (DMTA) of nanofilms and microfilms

DMTA tests were carried out to obtain the thermo-mechanical characteristics (storage modulus) of the produced CMF and CNF films. The test was performed in tension mode at a controlled heating rate of 5 °C/min. The temperature was raised from 30 °C to 250 °C at an oscillatory frequency of 1 Hz.

RESULTS AND DISCUSSION

Chemical properties

HPLC analyses

The glucan and xylan contents and material loss (%) after each pretreatment step are shown in Tables 2 and 3 for kraft and kraft-NaBH₄ pulps, respectively. The first mechanical refining slightly diminished the contents of glucan (2.56% and 1.45%) and xylan (0.31% and 1.63%) for o.d. bleached kraft and o.d. kraft-NaBH₄ pulps, respectively.

The refined samples were then enzymatically pretreated with Celluclast 1.5 L. Celluclast 1.5 L, which has been found to be effective in extracting glucose units from the fiber structure, mainly consists in cellulases or endo-glucanase units. It breaks down cellulosic materials in the cell walls and converts them to glucose by liberating glucose units. Csiszar *et al.*²⁷ studied the degradation effect of several enzymes on cotton fabric. They revealed that cellulase-based enzymes (Celluclast 1.5 L, Cellulase EBT, Cellusoft L) were effective in terms of mass loss and filter paper activity (FPA), using an agitation process of up to 2 h or without agitation, due to the fact that the enzymes degraded mainly surface fibrils, small protruding fibers and seed coat fragments. While the Pulpzyme HC 2500 enzyme was reported to have an effect only on xylan in both kraft pulp and NaBH₄-modified kraft pulp,^{28,31} the Celluclast 1.5 L enzyme effectively degraded both glucan and xylan in the present study. The increase in enzyme concentrations caused higher degradation (Table 2 b and c for kraft pulp, Table 3 b and c for kraft-NaBH₄ pulp). Celluclast 1.5 L exhibits hemicellulase activity provided by β-xylosidase, as well as cellulase activity.³² It was observed that the enzyme removed up to 21.1% of the glucan and 1.51% of the xylan from the structure of the o.d. bleached kraft pulp (Table 2c). On the other hand, 20.3% glucan and 31.0% xylan degradation was observed for the o.d. bleached kraft-NaBH₄ pulp (Table 3c). The higher degradation in the modified kraft pulp could be explained by the higher delignification, resulting in a more open structure to enzymatic activity.

Table 2
Changes in chemical components of bleached kraft pulp after mechanic/enzymatic pretreatments and homogenization

A	Chemical components (%)	Chip	Kraft	Kraft (ODEP)	1. Mechanical refining	Enzymatic treatment concentrations, EGU/g			Sample treated with optimum enzyme concentration (10 EGU/g)		
						2	5	10	2. Mechanical refining	CMF	CNF
						Glucan	40.0±1.53	61.8±2.04	66.3±0.90	65.7±0.01	64.7±0.15
Xylan	8.67±0.19	15.3±0.65	14.3±0.85	14.5±0.24	15.3±0.66	15.8±0.12	16.7±0.02	16.8±0.18	16.8±0.10	16.6±0.22	

B	% removed material (o.d. chip)	Chip	Kraft	Kraft (ODEP)	1. Mechanical refining	Enzymatic treatment concentrations, EGU/g			Sample treated with optimum enzyme concentration (10 EGU/g)		
						2	5	10	2. Mechanical refining	CMF	CNF
						Total material	-	54.4	58.5	59.2	61.5
Glucan	-	29.5	31.2	33.0	37.7	41.3	45.8	45.9	46.3	46.9	
Xylan	-	19.5	31.6	31.8	32.1	32.4	32.6	32.8	33.1	34.1	

C	% removed material (o.d. bleached kraft pulp)	Chip	Kraft	Kraft (ODEP)	1. Mechanical refining	Enzymatic treatment concentrations, EGU/g			Sample treated with optimum enzyme concentration (10 EGU/g)		
						2	5	10	2. Mechanical refining	CMF	CNF
						Glucan	-	-	-	2.56	9.47
Xylan	-	-	-	0.31	0.74	1.23	1.51	1.77	2.33	3.78	

Table 3
Changes in chemical components of bleached kraft-NaBH₄ pulp after mechanic/enzymatic pretreatments and homogenization

A	Chemical components (%)	Chip	Kraft-NaBH ₄	Kraft-NaBH ₄ (ODEP)	1. Mechanical refining	Enzymatic treatment concentrations, EGU/g			Sample treated with optimum enzyme concentration (2 EGU/g)		
						2	5	10	2.		
									Mechanical refining	CMF	CNF
	Glucan	40.0±1.53	62.6±0.98	66.2±0.81	65.9±0.14	64.3±0.55	62.0±0.14	62.0±0.88	65.0±0.12	64.8±0.42	64.7±1.01
	Xylan	8.67±0.19	15.8±0.65	15.8±0.85	15.7±0.32	16.3±0.91	13.7±0.34	12.8±0.47	16.9±0.45	16.4±0.38	16.3±0.55

B	% removed material (o.d. chip)	Chip	Kraft-NaBH ₄	Kraft-NaBH ₄ (ODEP)	1. Mechanical refining	Enzymatic treatment concentrations, EGU/g			Sample treated with optimum enzyme concentration (2 EGU/g)		
						2	5	10	2.		
									Mechanical refining	CMF	CNF
	Total material	-	54.7	60.5	60.9	63.8	64.7	66.4	65.3	65.4	65.6
	Glucan	-	29.1	34.6	35.6	41.9	45.3	47.9	43.7	44.0	44.3
	Xylan	-	17.4	28.0	29.2	32.0	44.3	50.3	32.5	34.6	35.2

C	% removed material (o.d. bleached kraft-NaBH ₄ pulp)	Chip	Kraft-NaBH ₄	Kraft-NaBH ₄ (ODEP)	1. Mechanical refining	Enzymatic treatment concentrations, EGU/g			Sample treated with optimum enzyme concentration (2 EGU/g)		
						2	5	10	2.		
									Mechanical refining	CMF	CNF
	Glucan	-	-	-	1.45	11.1	16.4	20.3	13.9	14.3	14.8
	Xylan	-	-	-	1.63	5.53	22.6	31.0	6.16	9.12	10.0

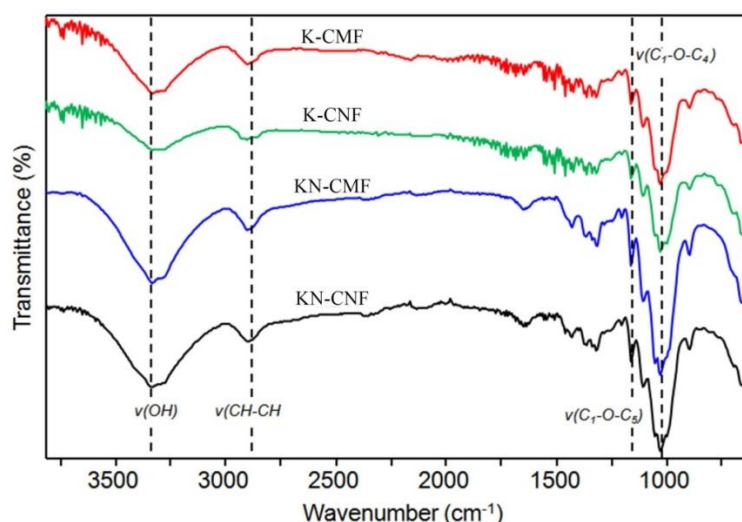


Figure 2: FTIR spectra of CMF/CNFs produced from kraft and kraft- NaBH_4 pulps (K: bleached kraft pulp, KN: bleached kraft- NaBH_4 pulp)

The optimum enzyme condition regarding the ratio of removed glucan to xylan should preserve more hemicelluloses in the structure and thus is expected to diminish cell wall cohesion and make cell wall delamination easier.³³ Consequently, it might prevent blocking in the homogenizer.³⁴ Therefore, the enzyme dose (Celluclast 1.5 L of 10 and 2 EGU/g for kraft and kraft- NaBH_4 pulps, respectively) that led to removing only 1.51% (Table 2c) and 5.53% (Table 3c) of the xylan from the o.d. bleached kraft and kraft- NaBH_4 pulps, respectively, was selected as the optimum for further analysis.

The samples were then mechanically refined again and the treatment resulted in almost no xylan or glucan degradation in the structure of the pulps. The homogenization process to obtain CMF and CNF indicated that only a slight amount of xylan and glucan was removed from the structure.³⁵

FTIR analyses

The molecular interactions related to CMF/CNFs produced from kraft and kraft- NaBH_4 pulps were investigated by FTIR and the results are given in Figure 2.

The broad O-H stretching peaks observed at 3328 cm^{-1} present the free OH groups of the nano- and micro-cellulose molecules, corresponding to intra- and intermolecular H-bonds.³⁶ The CNFs displayed lower transmittance, compared to the CMFs. The O-H in-plane bending and O-H bending vibration were additionally observed at 1336 cm^{-1} and 1202 cm^{-1} , respectively.³⁷ Likewise, those peaks presented the same reaction pattern as the O-H vibration at the 3328 cm^{-1} peak.

The CH_2 asymmetric stretching vibration was seen at around 2895 cm^{-1} .³⁸ The peaks observed at about 1200 and 1000 cm^{-1} represent the C-O-C vibrations in the cellulose structure. The peaks at about 1163 cm^{-1} are related to the $\text{C}_1\text{-O-C}_5$ asymmetric bridge stretching, which shows the ether linkage in the pyranose rings, while no significant shifts were observed in those peaks. In addition, the peaks observed at 1033 cm^{-1} show the glycosidic ($\text{C}_1\text{-O-C}_4$) deformation or pyranose ring skeletal vibration in the cellulose. When the CNFs were compared with the CMFs, the intensity of those peaks decreased. This finding showed higher degradation of the cellulose chains during CNF production.³⁹

It was observed that the NaBH_4 -modified kraft pulp led to much more disintegration and specific surface area due to the much greater area and increased peak intensity in all specific molecular interactions for the KN-CMF/CNF, compared to the K-CMF/CNF samples.^{36,40-43} Consequently, the NaBH_4 was found to have had an impact on the disintegration of the cellulose fibrils, thus making disintegration easier. On the other hand, similar vibrations were observed when using the Celluclast 1.5 L enzyme, compared to the use of the Pulpzyme HC 2500 enzyme, in the experiments carried out in our earlier studies.^{28,31}

^{13}C CP/MAS NMR analyses

The chemical structures of the samples were also analyzed by CP/MAS ^{13}C -NMR (Fig. 3). Chemical shifts were observed for both CMF and CNF produced from NaBH_4 -modified kraft pulp,

which could be attributed to the packing effect of the supramolecular structures as a result of the different chemical reactions applied.⁴⁴

The sharpest, most intense peaks were related to the C2, C3 and C5 positions, which were observed at around 59-52 ppm. In the spectra of both CMF and CNF produced from NaBH₄-modified kraft pulp, those were doubled collateral peaks, especially in the C3 and C5 positions. The C6 peaks could be seen at around 49-44 ppm. The C4 peaks at around 49-44 ppm provided insights into the crystalline (ordered) and non-crystalline (less ordered) forms, as the former (left) peak was thought to be crystalline in character, whereas the latter (right) showed an amorphous character.^{45,46}

The cellulose crystallinity index (CrI) calculated from the C4 peak signals (Table 4) is the simplest and also the most widely used, and involves the measurement of just two heights in the X-ray diffractogram. This produced a significantly higher crystallinity value than the ¹³C-NMR methods.⁴⁶ Therefore, the ¹³C-NMR spectroscopy techniques were evaluated in order to find a reliable crystallinity value.

Table 4
Crystallinity value of the samples

Sample	CrI
K-CMF	0.719
K-CNF	0.636
KN-CMF	0.619
KN-CNF	0.572

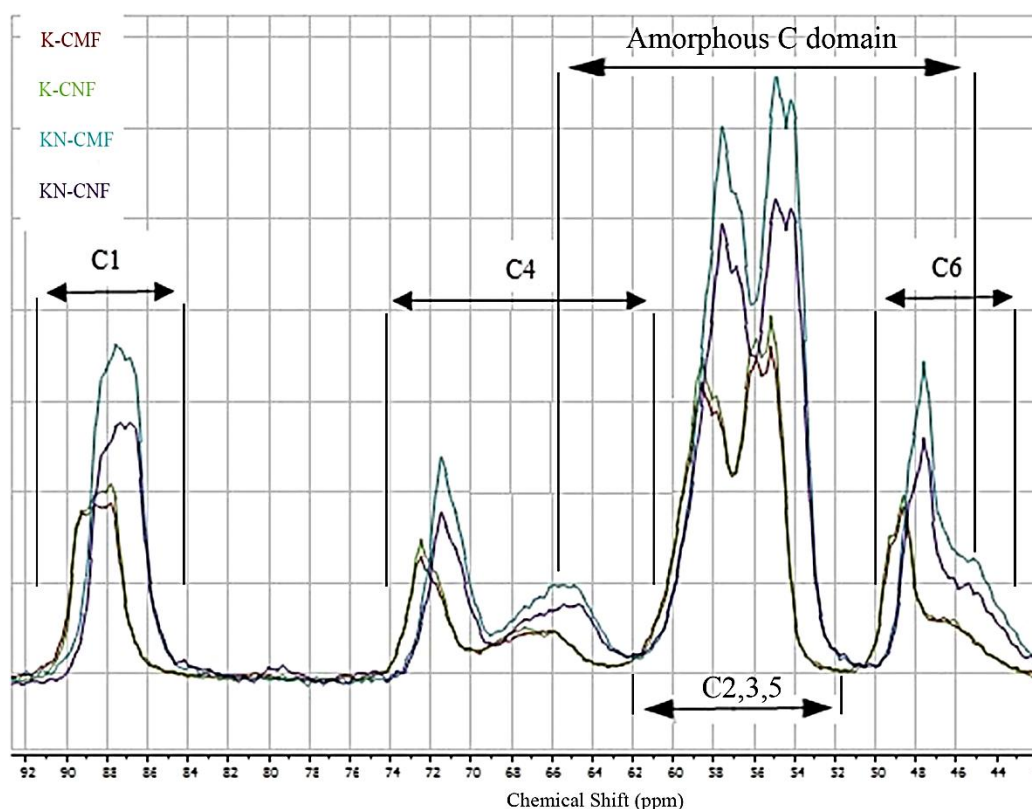


Figure 3: ¹³C-NMR spectra of CMF/CNFs produced from kraft and kraft-NaBH₄ pulps (K: bleached kraft pulp, KN: bleached kraft-NaBH₄ pulp)

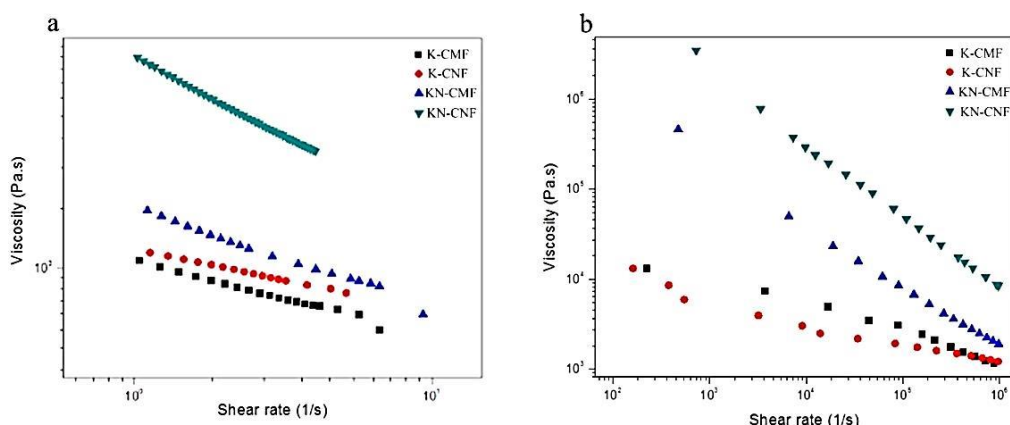


Figure 4: Viscosity as a function of shear rate for CMF/CNFs produced from kraft and kraft- NaBH_4 pulps (K: bleached kraft pulp, KN: bleached kraft- NaBH_4 pulp)

When the CNF and CMF samples were compared, there was a considerable decrease in the crystalline index value for the CNFs produced from both kraft and kraft- NaBH_4 pulps. These findings revealed that the application of the second chamber in the high-pressure homogenizer, with an orifice of 100 μm in diameter, caused the decreased crystallinity and produced more amorphous cellulose units for both pulps. Similar results were obtained by Nair *et al.*⁴⁷ This finding was supported by DSC analysis as well. In addition to FTIR, a similar reaction was observed in ^{13}C -NMR, in which a higher area and increased peak intensity was noted for the KN-CMF/CNF, compared to the K-CMF/CNF samples. Besides, no considerable differences in FTIR vibration and ^{13}C -NMR shifts were observed between the use of Celluclast 1.5 Land that of Pulpzyme HC 2500).^{28,31}

Rheological properties

The rheological properties of bio-based suspensions are of major importance for the prediction of composite performance for the potential end applications. The rheological properties provide an insight into the shear thinning or shear thickening behavior, which is widely influenced by the entanglement of the fibrillated fiber network.⁴⁸ In order to expound on these properties, viscosity was plotted as a function of the shear rate for the CMF and CNF samples obtained from both kraft and kraft- NaBH_4 pulps (Fig. 4).

The processed heterogeneous CMF and CNF suspensions contained fibers of different diameters and aspect ratios giving different viscosity values. An increase in shear rate decreased the viscosity of all suspensions. This showed the shear thinning behavior, and the materials tested in this study showed pseudoplastic behavior. These findings are in agreement with other studies in the literature.^{34,49}

The composition of the fibrils and the homogeneity of the fibril size distribution affected the viscosity of the CMF and CNF suspensions. A lower viscosity value was revealed by the low shear rate (1s^{-1} - 10s^{-1}) (Fig. 4a).⁵⁰ At a high shear rate value (Fig. 4b), CMF and CNF suspensions had a tendency to become unstable due to flocculation because thicker fibers got entangled in the thinner fiber network, forming big flocs, while the aggregation of single cellulose microfibrils occurred through the interaction of the thin fibers. Therefore, a descending rate of viscosity values occurred at the high shear rate (10^3s^{-1} - 10^6s^{-1}).

However, the decreasing trend of the viscosity was somewhat more stable for the samples produced from NaBH_4 -modified kraft pulp. A higher and more stable value was obtained with KN-CNF at low and high shear rates, whereas K-CNF revealed higher fluctuation at high shear rates as an indication of flocculation. Therefore, it can be assumed that NaBH_4 modification contributed as a stabilizer and led to a uniform production of fibers with a high surface area.⁵¹

Furthermore, the higher viscosity of CNF suspensions compared to CMF suspensions at equivalent concentrations is related to the higher number of hydrogen interactions and/or more important fiber entanglement. In all samples, processes of enzymatic and mechanical pretreatments followed by homogenization significantly diminished the viscosity of the samples. This decrease could be also explained by the increasing negative electrostatic charge, lower floc size, narrower size distribution or the gradual breaking of the 3D network as well as by the Einstein coefficient: higher length to

diameter ratio.⁵² Moreover, the use of the Celluclast 1.5 L enzyme led to a lower viscosity value of the kraft-NaBH₄ pulp, compared to the Pulpzyme HC 2500 enzyme.²⁸

Morphological (structural) properties

Figure 5 shows SEM images of the CMF and CNF samples produced from kraft and NaBH₄-modified kraft pulp. The SEM images of CMFs display nanofibrils and some micron-wide fibers. On the other hand, the SEM images of CNFs display no micron-wide fibers and the collected dispersion was fairly homogeneous.

The cellulosic nanofibers obtained from bleached kraft and kraft-NaBH₄ pulps in this study had an average length of 3347 nm ± 310 nm and 2940 nm ± 87 nm and a width of 31 nm ± 4 nm and 23 nm ± 3 nm, respectively. The average aspect ratios of the generated CNFs obtained from bleached kraft and kraft-NaBH₄ pulps were 110 ± 25 and 129 ± 20. Moon *et al.*⁵³ produced CNF with an aspect ratio of >100, a diameter of 4-10 nm and a length of several micrometers. The results showed that the CNF produced from modified kraft pulp resulted in smaller-sized nanofibrils, compared to that of the kraft pulp. This finding could be explained the higher hemicellulose content of the modified kraft pulp. The higher hemicellulose might have decreased the cell wall cohesion and made cell wall delamination easier.^{33,34} In the literature, CNFs of about 10-100 nm were produced by different techniques.^{54,55} The results obtained indicate that the use of Celluclast 1.5 L enabled achieving fibrils with smaller dimensions from both pulps, in comparison with the use of PulpzymeHC 2500.^{28,31}

Thermal characterization

The DSC thermograms for the CMF and CNF samples obtained from both kraft and kraft-NaBH₄ pulps are shown in Figure 6. Considerable endothermic peaks at around 340 °C to 380 °C can be observed.⁴¹

The endotherm is an indication of the fusion or melting process that can give an idea about the nature of crystalline packing, the extent to which it increases or its prominence in going from the precursor to the corresponding nanocellulose, and the nature of the amorphous regions during the fusion process.⁵⁶

The peaks also indicate the degree of cellulose decomposition. The increasing degradation temperature was associated with higher thermal stability, and this behavior has been attributed to the high degree of material crystallinity.⁵⁷

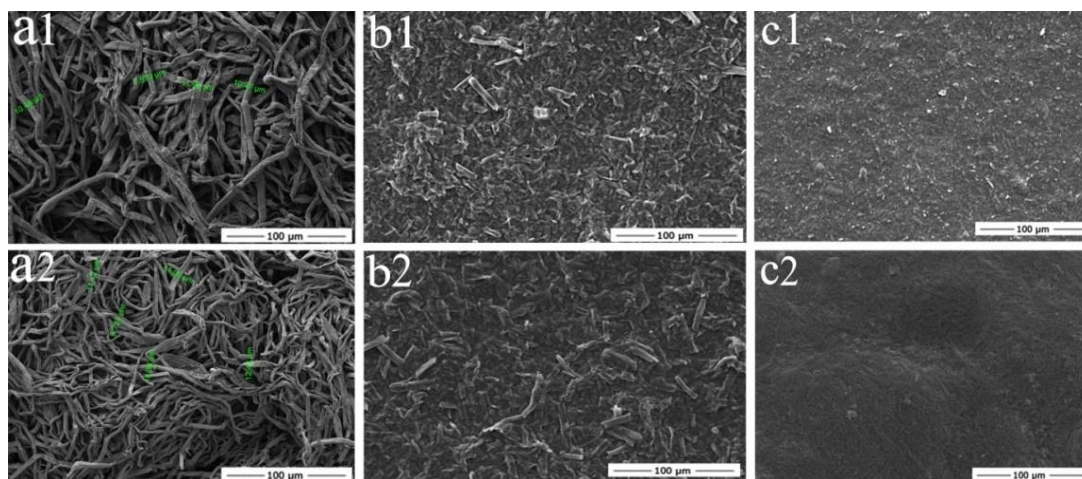


Figure 5: SEM images for: (a1) bleached kraft pulp (K), (b1) K-CMF, (c1) K-CNF, (a2) bleached kraft-NaBH₄ pulp (KN), (b2) KN-CMF and (c2) KN-CNF materials

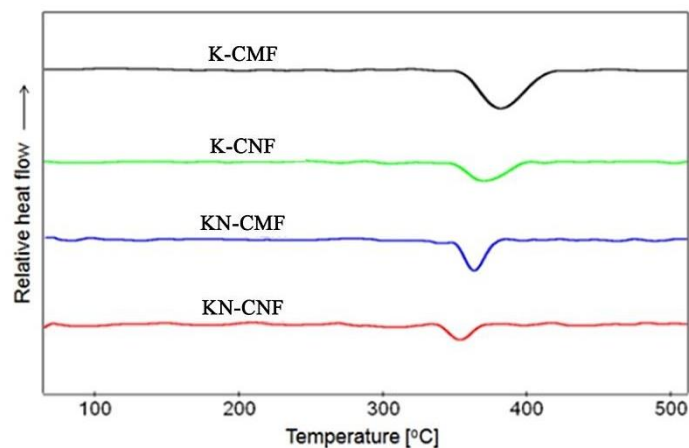


Figure 6: DSC curves for 25-500 °C of CMF/CNFs produced from kraft and kraft- NaBH_4 pulps (K: bleached kraft pulp, KN: bleached kraft- NaBH_4 pulp)

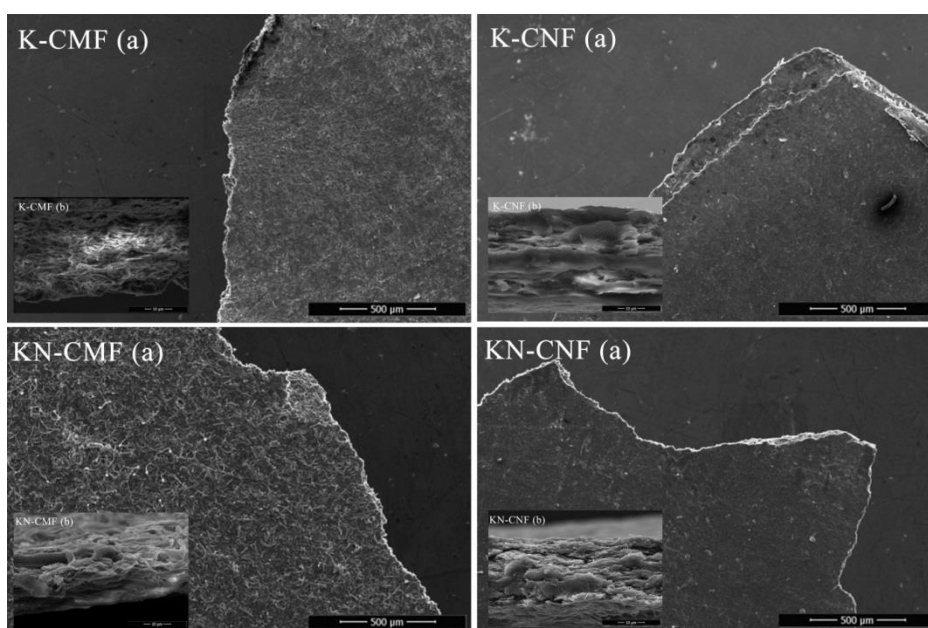


Figure 7: SEM images of (a) surface and (b) cross-section of CMF or CNF films (K: bleached kraft pulp, KN: bleached kraft- NaBH_4 pulp)

It was observed that the CMF suspensions degraded progressively to a greater extent, compared to the CNF suspensions. This findings could be due to the degradation of the glycosidic bonds of cellulose and to the fibrillation inducing the crystalline/amorphous ratio in the structure.⁵⁸ In addition, it could be said that the second chamber with an orifice of 100 μm in the high-pressure homogenizer caused more fibrillation, thus increasing the amorphous structure. Also, these findings correlated with the ^{13}C -NMR results. In addition, the lower thermal stability was seen in the suspensions produced from NaBH_4 treated kraft pulps. This probably stems from the lower glucan ratio of the modified kraft pulp.

Dynamic mechanical thermal analysis (DMTA)

Figure 7 shows the surface (a) and the cross-section (b) SEM images of the fractured films. The surface of the CNF films was smoother and the cross-section more homogeneous, compared to those of the CMF films. It should also be mentioned that the CNF films had much more uniform dispersion than the CMF films. The less durable form of the CMF films led to early breakage during DMTA analyses; therefore, no storage modulus value was obtained for these films.

Storage modulus as a viscoelastic performance parameter is of great importance to the nanofilms used in biomedical, food packaging, electronics and many other applications. The viscoelasticity of the

nanocomposites can be efficiently evaluated by DTMA as a function of temperature. The dependence of dynamic mechanical thermal behaviors on temperature for cellulose-based nanofilms in the temperature range of 20 °C to 220 °C is presented in Figure 8.

The curves acquired from the DMTA analysis indicated that the storage modulus values of the KN-CNF and K-CNF films made from nanocellulose increased with increasing temperature from 30 °C to 136 °C and 30 °C to 101 °C, respectively. After reaching the maximum value, the storage modulus values of the nanofilms made from nanocellulose decreased with the increasing temperature up to 230 °C. Figure 8 illustrates that the storage modulus values of the KN-CNF and K-CNF films made from nanocellulose at the minimum temperature were 1.88 GPa and 6.97 GPa, respectively, while the storage modulus values at the maximum temperature were 4.14 GPa and 6.13 GPa, respectively. In addition, the maximum storage modulus values of the KN-CNF and K-CNF films made from nanocellulose were found to be 5.43 GPa and 9.71 GPa, respectively. Honorato *et al.*⁵⁹ examined the mechanical properties of TEMPO-oxidized CNF films produced from eucalyptus fibers and found the storage modulus of the nanofilms to be 7.20 GPa.

It was determined that the initial and final storage modulus values of the K-CNF films were improved by 270% and 48%, respectively. In addition, the maximum storage modulus values were increased by 78%. The results clearly showed that the overall and high temperature performances of the K-CNF film were higher than those for the KN-CNF films. This can be explained by the fact that the values of removed glucan and xylan differed in the present study, while these removed contents and the initial ones affected significantly the mechanical values of the films. In the kraft-NaBH₄ pulp, the removal of xylan is considerably higher than in the kraft pulp subjected to enzymatic pretreatment. As a result, it was observed that the storage modulus of the film produced from kraft-NaBH₄ pulp is lower by nearly 40%. The results obtained in this study were consistent with the findings of Arjmandi *et al.*⁶⁰ They reported that the higher performance of cellulose nanowhiskers as nanofillers was due to an enhanced stress transfer. Thus, the modulus of the composite was higher than that of the microcellulose fibers. When considering the effect of the enzyme on the storage modulus of the films, it can be noted that a lower value was obtained for the Celluclast 1.5 L treated sample, compared to the results reported earlier for the use of PulpzymeHC 2500.²⁸

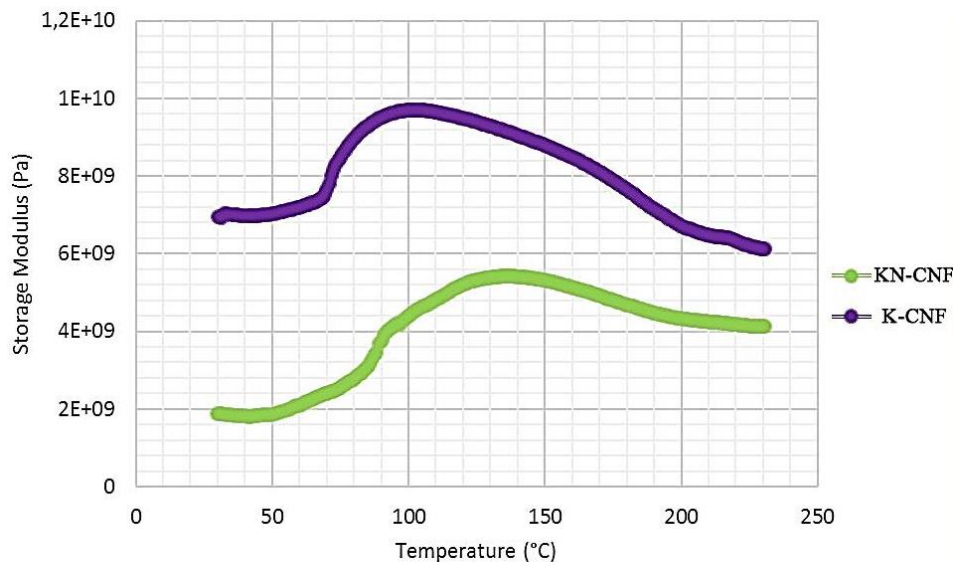


Figure 8: Storage modulus curves of CNF films (K: bleached kraft pulp, KN: bleached kraft-NaBH₄ pulp)

CONCLUSION

In this study, CMF and CNF were prepared from kraft and kraft-NaBH₄ pulp by using Celluclast 1.5 L enzyme to lower the energy input ahead of high-pressure fibrillation. To date, the effect of this enzyme when used for this purpose has not been sufficiently studied. Celluclast 1.5 L effectively degraded the glucan in the structure of the pulps. Major shifts were observed in ¹³C-NMR for the CMF/CNF obtained from modified kraft pulp due to the chemical reactions of the NaBH₄ reducing agent. When fluid properties were examined, shear thinning behavior was observed in all the samples,

while the CNF obtained from kraft pulp had the lowest viscosity value. The CMF and CNF obtained from kraft pulp exhibited higher crystallinity values and thermal stability. The NaBH₄ caused a negative effect on thermal stability. The SEM pictures revealed that the CNF produced from NaBH₄-modified kraft pulp resulted in smaller-sized nanofibrils. The films produced from CNF were examined *via* DMTA and the results showed that the overall and high temperature performances of the CNF film obtained from kraft pulp were higher than those of the CNF film obtained from NaBH₄-modified kraft pulp. The maximum storage modulus value of the CNF film obtained from kraft pulp was found to be 9.71 GPa. It is thought that these nanocomposites can be easily used in many applications.

ACKNOWLEDGEMENT: The authors thank TUBITAK (Project Number: COST 114O022) for support in this research. The authors also thank Istanbul University Research Fund for its financial support in this study (Project Number: 4806 and Project Number: 19515).

REFERENCES

- ¹ A. Mandal and D. Chakrabarty, *Carbohydr. Polym.*, **86**, 1291 (2011).
- ² K. R. Sandberg, F. W. Snyder and A. F. Turbak, US Patent US GB2066145 A, 1981.
- ³ A. F. Turbak, F. W. Snyder and K. R. Sandberg, *J. Appl. Polym. Sci., Appl. Polym. Symp.*, **37**, 815 (1983).
- ⁴ G. Garrasco, *Nanoscale Res. Lett.*, **6**, 417 (2011).
- ⁵ V. Kumar, R. Bollström, A. Yang, Q. Chen, G. Chen *et al.*, *Cellulose*, **21**, 3443 (2014).
- ⁶ P. Kleinebudde, *AAPS Pharm. Sci.*, **2**, 1 (2000).
- ⁷ J. Han, C. Zhou, Y. Wu, F. Liu and Q. Wu, *Biomacromolecules*, **14**, 1529 (2013).
- ⁸ F. Curtol and N. C. Eksteen, US Patent US 20060006189 A1, 2006.
- ⁹ B. Langlois, J. Benchimol, G. Guerin, I. Vincent, A. Senechal *et al.*, US Patent US 6348436 B1, 2002.
- ¹⁰ W. V. Klemp, P. M. Ducker, S. W. Sneed and M. Suzuki, US Patent US 20040193128 A1, 2004.
- ¹¹ P. K. Chatterjee and K. B. Makoui, US Patent US 4474949 A, 1983.
- ¹² L. Mondet, US Patent US 6001338A, 1999.
- ¹³ S. Innami and Y. Fukui, US Patent US 4659388 A, 1987.
- ¹⁴ A. F. Turbak, A. El-Kafrawy, F. W. Snyder and A. B. Auerbach, US Patent US 4352770 A, 1982.
- ¹⁵ J. Y. Cavaille, A. Dufresne, M. Paillet, M. A. S. Azizi Samir, F. Alloin *et al.*, US Patent US 20060102869 A, 2006.
- ¹⁶ J. Li, Z. Song, D. Li, S. Shang and Y. Guo, *Ind. Crop. Prod.*, **59**, 318 (2014).
- ¹⁷ A. N. Nakagaito and H. Yano, *Appl. Phys. A*, **78**, 547 (2004).
- ¹⁸ M. G. Thomas, E. Abraham, P. Jyotishkumar, H. J. Maria, L. Pothen *et al.*, *Int. J. Biol. Macromol.*, **81**, 768 (2015).
- ¹⁹ M. A. S. Azizi Samir, F. Alloin, M. Paillet and A. Dufresne, *Macromolecules*, **37**, 4313 (2004).
- ²⁰ Y. Shimazaki, Y. Miyazaki, Y. Takezawa, M. Nogi, K. Abe *et al.*, *Biomacromolecules*, **8**, 2976 (2007).
- ²¹ F. Grüneberg, T. Künniger, T. Zimmermann and M. Arnold, *J. Mater. Sci.*, **49**, 6437 (2014).
- ²² N. Lavoine, I. Desloges, A. Dufresne and J. Bras, *Carbohydr. Polym.*, **90**, 735 (2012).
- ²³ T. Taniguchi and K. Okamura, *Polym. Int.*, **47**, 291 (1998).
- ²⁴ Y. Matsuda, M. Hirose and K. Ueno, US Patent US 6214163 B1, 2001.
- ²⁵ A. Alemdar and M. Sain, *Bioresour. Technol.*, **99**, 1664 (2008).
- ²⁶ B. Wang and M. Sain, *Compos. Sci. Technol.*, **67**, 2521 (2007).
- ²⁷ E. Csizsar, K. Urbanszki and G. Szakacs, *J. Mol. Catal. B: Enzym.*, **11**, 1065 (2001).
- ²⁸ A. Tozluoglu, B. Poyraz, Z. Candan, M. Yavuz and R. Arslan, *Bull. Mater. Sci.*, **40**, 699 (2017).
- ²⁹ A. Sluiter, B. Hames, R. Ruiz, C. Scarlata, J. Sluiter *et al.*, Determination of structural carbohydrates and lignin in biomass. Biomass Analysis Technology Team Laboratory Analytical Procedures, National Renewable Research Laboratory, Golden, CO, USA, 2004.
- ³⁰ D. Trache, A. Donnot, K. Khimeche, R. Benelmir and N. Brosse, *Carbohydr. Polym.*, **104**, 223 (2014).
- ³¹ A. Tozluoglu, B. Poyraz and Z. Candan, *Maderas Cienc. Tecnol.*, **20**, 67 (2018).
- ³² M. A. Khan, Master Thesis, Lulea University of Technology, Sweden, 2010.
- ³³ R. Kolakovic, PhD Thesis, Division of Pharmaceutical Technology, Faculty of Pharmacy, University of Helsinki, Helsinki, Finland, 2013.
- ³⁴ M. Pääkko, M. Ankerfors, H. Kosonen, A. Nykänen, S. Ahola *et al.*, *Biomacromolecules*, **8**, 1934 (2007).
- ³⁵ S. Virtanen, J. Vartianen, H. Setälä, T. Tammelin and S. Vuoti, *RSC Adv.*, **4**, 11343 (2014).
- ³⁶ H. M. Ng, L. T. Sin, T. T. Tee, S. T. Bee, D. Hui *et al.*, *Compos. Part B Eng.*, **75**, 176 (2015).
- ³⁷ M. Jonoobi, K. O. Niska, J. Harun, A. Shakeri and M. Misra, *BioResources*, **4**, 626 (2009).
- ³⁸ M. Poletto, V. Pistor and A. J. Zattera, *Materials*, **7**, 6105 (2014).
- ³⁹ S. Y. Oh, D. I. Yoo, Y. Shin and G. Seo, *Carbohydr. Res.*, **340**, 417 (2005).

- ⁴⁰ E. Abraham, B. Deepa, L. A. Pothan, J. Cintil, S. Thomas *et al.*, *Carbohydr. Polym.*, **92**, 1477 (2013).
- ⁴¹ A. Mandal and D. Chakrabarty, *Carbohydr. Polym.*, **86**, 1291 (2011).
- ⁴² T. N. Ang, G. C. Ngoh, A. S. M. Chua and M. G. Lee, *Biotechnol. Biofuels*, **5**, 67 (2012).
- ⁴³ F. Jiang and Y. L. Hsieh, *Carbohydr. Polym.*, **95**, 32 (2013).
- ⁴⁴ G. Zuckerstätter, G. Schild, P. Wollboldt, T. Röder, H. Weber *et al.*, *Lenzinger Ber.*, **87**, 38 (2009).
- ⁴⁵ R. H. Newman, *Cellulose*, **11**, 45 (2004).
- ⁴⁶ S. Park, J. O. Baker, M. E. Himmel, P. A. Parilla and D. K. Johnson, *Biotechnol. Biofuels*, **3**, 10 (2010).
- ⁴⁷ S. S. Nair, J. Y. Zhu, Y. Deng and A. J. Ragauskas, *J. Nanopart. Res.*, **16**, 2349 (2014).
- ⁴⁸ T. Saito, Y. Nishiyama, J. Putaux, M. Vignon and A. Isogai, *Biomacromolecules*, **7**, 1687 (2006).
- ⁴⁹ M. Iotti, Ø. Gregersen, S. Moe and M. Lenes, *J. Polym. Environ.*, **19**, 137 (2011).
- ⁵⁰ H. Taheri and P. Samyn, *Cellulose*, **23**, 1221 (2016).
- ⁵¹ S. Iwamoto, A. N. Nakagaito and H. Yano, *Appl. Phys. A*, **89**, 461 (2007).
- ⁵² A. Dufresne, “Nanocellulose: From Nature to High Performance Tailored Materials”, Grenoble, Walter de Gruyter, Chapter 6, 2012.
- ⁵³ R. J. Moon, A. Martini, J. Nairn, J. Simonsen and J. Youngblood, *Chem. Soc. Rev.*, **40**, 3941 (2011).
- ⁵⁴ M. Ankerfors, T. Lindström and G. Henriksson, US Patent US 20090221812 A1, 2009.
- ⁵⁵ J. Leitner, B. Hinterstoisser, M. Wastyn, J. Keckes and W. Gindl, *Cellulose*, **14**, 419 (2007).
- ⁵⁶ S. Maiti, J. Jayaramudu, K. Das, S. M. Reddy, R. Sadiku *et al.*, *Carbohydr. Polym.*, **98**, 562 (2013).
- ⁵⁷ S. F. S. Draman, R. Daik, F. A. Latif and S. M. El-Sheikh, *BioResources*, **9**, 8 (2014).
- ⁵⁸ T. Hosoya and S. Sakaki, *ChemSusChem*, **6**, 2356 (2013).
- ⁵⁹ C. Honorato, V. Kumar, J. Liu, H. Koivula and C. Xu, *J. Mater. Sci.*, **50**, 7343 (2015).
- ⁶⁰ R. Arjmandi, A. Hassan, S. Eichhorn, M. K. Mohamad Haafiz, Z. Zakaria *et al.*, *J. Mater. Sci.*, **50**, 3118 (2015).